Asian Review of Environmental and Earth Sciences
Vol. 7, No. 1, 61-66, 2020
ISSN(E) 2313-8173 / ISSN(P) 2518-0134
DOI: 10.20448/journal.506.2020.71.61.66

Spatio-temporal Analysis of Urban Built-up Land in the Hanoi Metropolitan Area (Vietnam) using Remotely Sensed Images

Thanh Tien Nguyen

Faculty of Surveying, Mapping and Geographic Information, Hanoi University of Natural Resources and Environment, Hanoi, Vietnam.
Email: tdgis_ntthanh@163.com Tel: +84975398584

Abstract

Rapid and unplanned urbanization leads to temperature rise, urban vegetation decrease, and built-up land increase, forming an urban heat island. It is, therefore, the change of built-up land plays an important role in surface urban heat island studies. This study aims to analyze spatio-temporal changes of urban built-up land in the Hanoi Metropolitan Area (HMA), Vietnam, using Landsat remotely sensed images acquired in 1996 and 2016. Landsat time-series images were first pre-processed preprocessed to account for sensor, solar, atmospheric, and topographic effects. Urban built-up land was then extracted based on an NDBI based continuous built-up index (BUc). Spatio-temporal changes of built-up land were finally analyzed by means of Geographic Information System (GIS). It was found that the urban built-up land area had increased from 4063.1 hectares in 1996 to 7163.2 hectares in 2016 which account for 13.3% and 23.4% of the total area, respectively. The built-up land area had increased by about 10.1% of the total area in 20 years. On average, 0.5% of the urban built-up area increases each year. The urban built-up land tends to expand to the west, southwest, and south of the HMA. These findings demonstrate the effectiveness of the proposed method for spatio-temporal analysis of built-up land in urban areas using remotely sensed images.

Keywords: Spatio-temporal analysis, Change detection, Urban built-up land, remotely sensed data, Landsat time-series images, Urban heat islands; Hanoi metropolitan area (Vietnam).

Citation | Thanh Tien Nguyen (2020). Spatio-temporal Analysis of Urban Built-up Land in the Hanoi Metropolitan Area (Vietnam) using Remotely Sensed Images. Asian Review of Environmental and Earth Sciences, 7(1): 61-66.
History:
Received: 17 February 2020
Revised: 20 March 2020
Accepted: 22 April 2020
Published: 25 May 2020

Publisher: Asian Online Journal Publishing Group

Funding: This study received no specific financial support.
Competing Interests: The author declares that there are no conflicts of interests regarding the publication of this paper.
Transparency: The author confirms that the manuscript is an honest, accurate, and transparent account of the study was reported; that no vital features of the study have been omitted; and that any discrepancies from the study as planned have been explained.
Ethical: This study follows all ethical practices during writing.

Contents

Contribution of this paper to the literature

This study provides the scientific basis for the spatio-temporal analysis of urban built-up land in urban areas through Landsat time-series images. In addition, this research can contribute a baseline for further empirical researches in the area of urban heat island studies in the Hanoi Metropolitan Area, Vietnam.

1. Introduction

Land covers in urban areas tend to change more drastically over a short period of time than elsewhere because of incessant urbanization [1]. Rapid development in urban areas has brought land cover change, especially built-up land urban in areas in such a developing country as Vietnam. The replacement of vegetation cover with urban built-up land caused by urbanization has led to negative environmental repercussions to urban areas [2], such as reduced precipitation [3, 4] more dryness [2] and warmer temperatures [5] which contribute greatly to atmospheric and urban heat islands. Built-up land in urban areas has been considered as an effective indicator of urban development and environmental quality. Recent studies have also shown that the increase of built-up land has resulted in serious negative effects on humans and environments such as the weakening of living environments and an increased mortality rate [6] the adverse health effects [7] and the worsening local weather and climate [8]. It is, therefore, the spatio-temporal analysis of urban built-up land change plays an important role in urban environmental studies.

Traditionally, manual interpretation of aerial photography or field surveys have been commonly used for built-up land change detection [9, 10]. The main advantage of these conventional methods is that built-up land could be captured with a high accuracy [11] but they were nearly impossible to gather enough data over a large area [12, 13] especially for such big urban areas as megacities. The occurrences of remote sensing technology now have overcome most of these limitations of conventional methods. Digital remotely sensed images allow for mapping urban areas and detecting land-use change in a more timely, cheaper and more accurate manner, especially when using the most recent high-resolution satellite imagery [11]. Since remotely sensed imagery of high-resolution satellite sensors such as Landsat-1, 2, 3 MSS, -5 TM, -7 ETM+ and -8 OLI started to become available, built-up land change detection and monitoring from space became easier. A commonly used approach for the definition of built-up land areas is conventional multi-spectral classification [2]. However, due to spectral confusion of the heterogeneous built-up land class, Xu [2] concluded that this method may not produce satisfactory accuracy. Therefore, many indices were proposed to discriminate built-up land from non-built-up land in urban areas such as the Normalised Difference Vegetation Index (NDVI) [14] Normalised Difference Built-Up Index (NDBI) [1], Index-based Built-Up Index (IBI) [2], Urban Index (UI) [15], Enhanced Built-Up and Bareness Index (EBBI) [16], vegetation index built-up index (VIBI) [17], a NDBI based continuous built-up index (BU_c) [18], and most recently, dry built-up index (DBI) [19]. The reviewed literature on spectral indices leads [19] to conclude that these indices have not entirely successfully addressed the confusion between impervious surfaces and bare soil. Commonly used NDBI and UI indices are unable to verify the distribution of built-up versus bare land areas As-syakur, et al. [16]. He, et al. [18] indicated that BU_c is considered the most effective index for mapping built-up land. Hence, by employing the BU_c, this study focusses on detecting the spatio-temporal change of urban built-up land in the Hanoi Metropolitan Area (Vietnam).

2. Study Area and Data Used

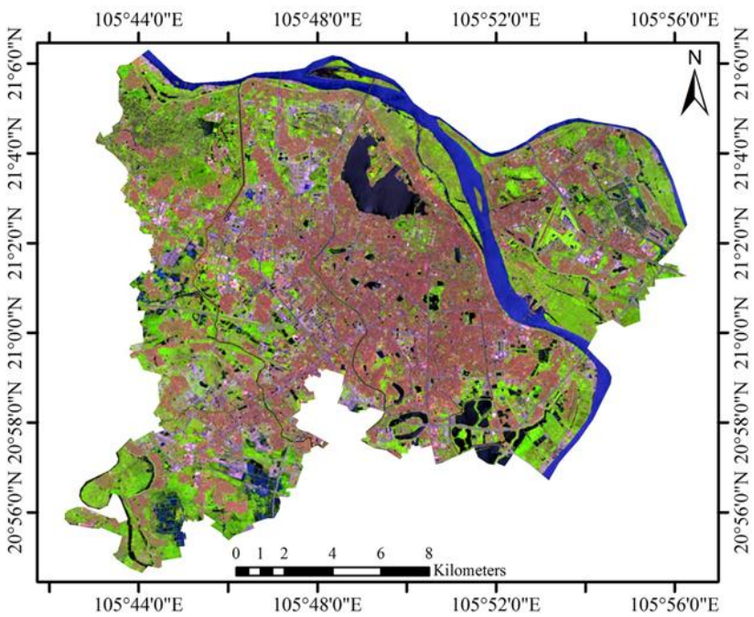

Figure-1. Study area of the HMA: 6-5-4 false color composite of Landsat-8 OLI images.

The HMA is located in the center of Hanoi capital of Vietnam. Its geographic location extends latitudinally from 20°54'34.14" to 21°6'22.69", and longitudinally from 105°42'16.97" to 105°56'21.48" Figure 1 covering an area of about 274 km². Hanoi, one of the largest cities in Vietnam with an estimated population of 8.05 million and a population density of 2,300 people for every square kilometer in 2019, undergoes a rapid urbanization, especially after the Doi Moi Policy in 1986. Rapid urbanization has caused vegetation to be replaced by built-up land dramatically [20]. Landsat-5 and 8 time-series images (path 127, row 045/046) with 30-m spatial resolution of

distributed by the U.S. Geological Survey were used in this study. These images were acquired on 10 June 1996 and on 16 May 2016. The quality of all Landsat images was rather good (9/9) with no cloud cover over in the HMA. Landsat image processing was carried out in the Environment for Visualizing Images software: ENVI version 5.2. Maps were produced by ArcGIS 10.2 software [21].

3. Methodology

3.1. Remotely Sensed Image Pre-Processing

The pre-processing of Landsat images includes two main steps. The conversion of the digital number data (Q_{cal}) to top of atmosphere (ToA or at-sensor) radiance ($L_{ToA,\lambda}$) is first performed using calibration parameters provided in the metadata file. The Q_{cal}-to-$L_{ToA,\lambda}$ conversion for Landsat-5 TM image and Landsat-8 OLI image [22] are conducted by means of Equations 1 and 2 respectively:

$$L_{ToA,\lambda} = \left(\frac{L_{max,\lambda} - L_{min,\lambda}}{Q_{cal\_max} - Q_{cal\_min}}\right) \times (Q_{cal} - Q_{cal\_min}) + L_{min,\lambda} \quad (1)$$

where $L_{TOA,\lambda}$ is at-sensor spectral radiance [$W/m^2.sr.\mu m$] at the wavelength λ (μm); Q_{cal} is digital number values; Q_{cal_min} and Q_{cal_max} are minimum and maximum digital number corresponding to $L_{min,\lambda}$ and $L_{max,\lambda}$, respectively; $L_{min,\lambda}$ and $L_{max,\lambda}$ are at-sensor spectral radiance [$W/m^2.sr.\mu m$].

$$L_{ToA,\lambda} = M_L Q_{cal} + \Delta_L \quad (2)$$

where $L_{ToA,\lambda}$ is at-sensor spectral radiance [$W/(m^2 \cdot sr \cdot \mu m)$] at the wavelength λ (μm); M_L and Δ_L are the radiance multiplicative scaling factor and the radiance additive scaling factor for the bands, respectively; and Q_{cal} is the digital number.

After the Q_{cal}-to-$L_{ToA,\lambda}$ conversion, atmospheric effects for Landsat-5 and 8 reflective bands is then carried out using FLAASH algorithm proposed by Adler-Golden, et al. [23]. The spectral radiance of Landsat bands in FLAASH model is identified based on the Equation 3 [23]:

$$L^* = \left(\frac{A\rho}{1-\rho_e S}\right) + \left(\frac{B\rho_e}{1-\rho_e S}\right) + L_a^* \quad (3)$$

where ρ is the surface reflectance of a pixel; ρ_e is the average surface reflectance for the pixel and surrounding pixels; S is the spherical albedo of the atmosphere; L_a^* is the radiance back-scattered by the atmosphere; A and B are coefficients depending on atmospheric and geometric conditions. The values of A, B, S, and L_a^* are obtained based on MODTRAN4 model [24]. After the water retrieval, the spatially averaged reflectance ρ_e is identified using the following equation [23, 24]:

$$L_e = \left(\frac{(A+B)\rho_e}{1-\rho_e S}\right) + L_a^* \quad (4)$$

where L_e *is* spatially averaged reflectance; A, B, S L_a^* and ρ_e are defined as in Equation 3.

3.2. Built-Up Land Extration from Landsat Images

The NDVI is considered as an indication of the presence of vegetation and amount or condition of vegetation on pixel basis [6, 25], whereas, the NDBI is an index for mapping built-up land [24]. In this study, the continuous built-up index (BU_c) proposed by He, et al. [18] which is based on NDVI and NDBI indices was employed to extract urban built-up land. These indices are estimated from Landsat bands using Equations 5, 6 and 7, respectively:

$$NDVI = \frac{R_{NIR} - R_{RED}}{R_{NIR} + R_{RED}} \quad (5)$$

$$NDBI = \frac{R_{MIR} - R_{NIR}}{R_{MIR} + R_{NIR}} \quad (6)$$

$$BU_c = NDBI - NDVI \quad (7)$$

where R_{RED}, R_{NIR}, and R_{MIR} are the ground reflectance of Landsat-5 TM band 3 of and Landsat-8 OLI band 4, of Landsat-5 TM band 4 and Landsat-8 OLI band 5, and of Landsat-5 TM band 5 and Landsat-8 OLI band 6, respectively. The BU_c is the resultant binary image with only the built-up and barren pixels having positive value, thus allowing built-up areas to be mapped automatically [1].

3.3. Spatio-Temporal Analysis of Built-Up Land Changes

After urban built-up land is extracted from Landsat-5 and -8 images at two-time points, the change of urban built-up land is detected with the help of GIS by means of ArcGIS software. In which, ArcGIS software helps to determine the built-up area, the percentage and spatial distribution during the period in the study area. Spatio-temporal changes of built-up land were finally analyzed and discussed by comparing with previous findings.

4. Results and Discussion

4.1. NDBI in 1996 and 2016

The NDBI distribution in the HMA obtained from Landsat-5 TM and -8 OLI images acquired on 10 June 1996 and 16 May 2016 are shown in Figure 2, whereas it's statistics are summarized in Table 1. Data from Table 1 illustrates that it's minimum, mean and maximum values of the NDBI computed from 1996 Landsat-5 TM image were -0.77, -0.07 and 0.56, respectively. Whereas, the minimum, mean and maximum values of the NDBI retrieved from 2016 Landsat-8 OLI were -0.45, 0.02 and 0.58, respectively. It can be seen that the NDBI values of 2016 were larger than those of 1996. This shows that the built-up land has increased in the period 1996-2016. Small areas of

high NDBI values were detected in the core urban areas of the HMA in 1996 Figure 2, left. However, these areas of high NDBI values had greatly expanded towards the western, north-western and south-western parts of the core urban HMA Figure 2, right. The rapid expansion of high NDBI value areas during the period of 1996-2016 was due to the high rate of urbanization after the Doi Moi policy [26]. Data from histograms in Figure 3 demonstrates that the distribution of the NDBI in 1996 was left-skewed with a relatively high number of low NDBI values Figure 3, left, however, this trend had changed in 2016. The NDBI in 2016 shows the number of pixels with NDBI values had increased much stronger than that of 1996. Nguyen, et al. [20] reported that the NDBI had been increasing dramatically in the period of 1996-2007. It can be concluded from the above-discussion that NDBI values had been increased in the period of 1996-2016.

Table-1. Descriptive statistics of the NDBI, BU_c in the HMA.

Index	Date	Minimum	Mean	Maximum	Standard deviation
NDBI	1996-6-10	-0.77	-0.07	0.56	0.02
	2016-5-16	-0.45	0.02	0.58	0.17
BU_c	1996-6-10	-1.00	0.53	0.94	0.41
	2016-5-16	1.00	0.58	1.00	0.40

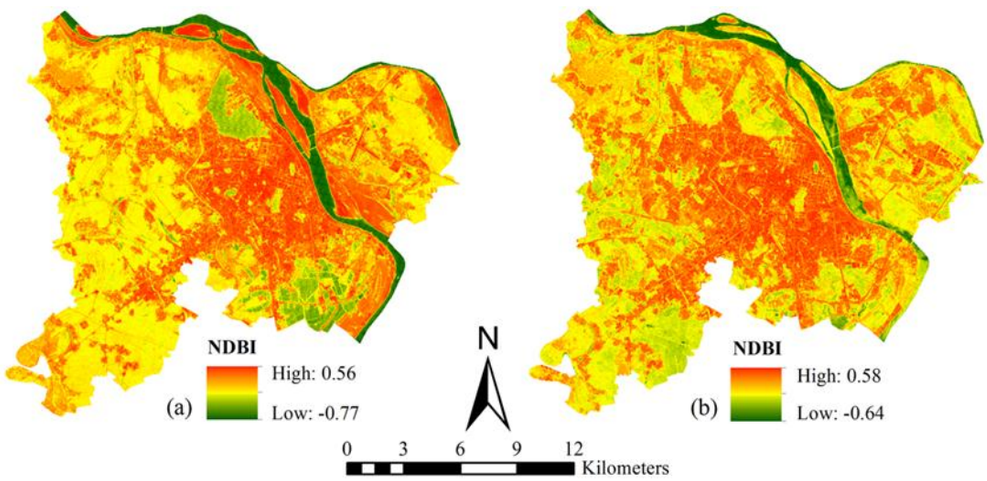

Figure-2. NDBI in the HMA in 1996 (a) and 2016 (b).

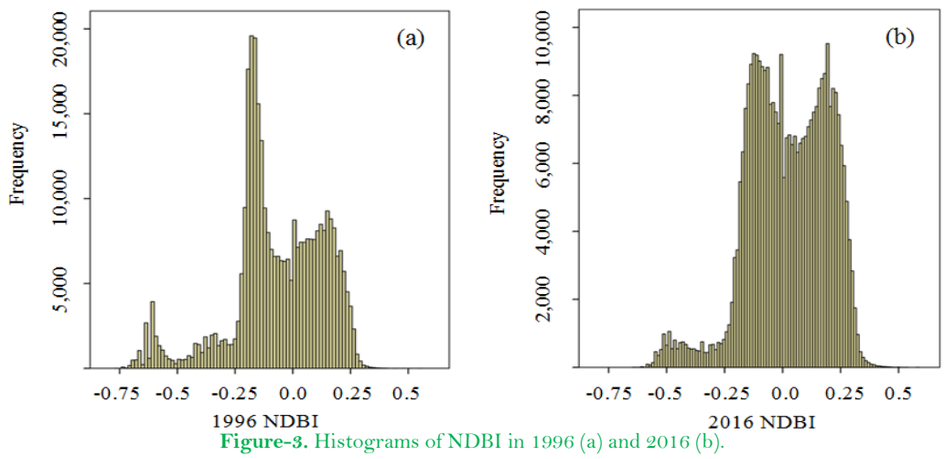

Figure-3. Histograms of NDBI in 1996 (a) and 2016 (b).

4.2. BU_c in 1996 and 2016

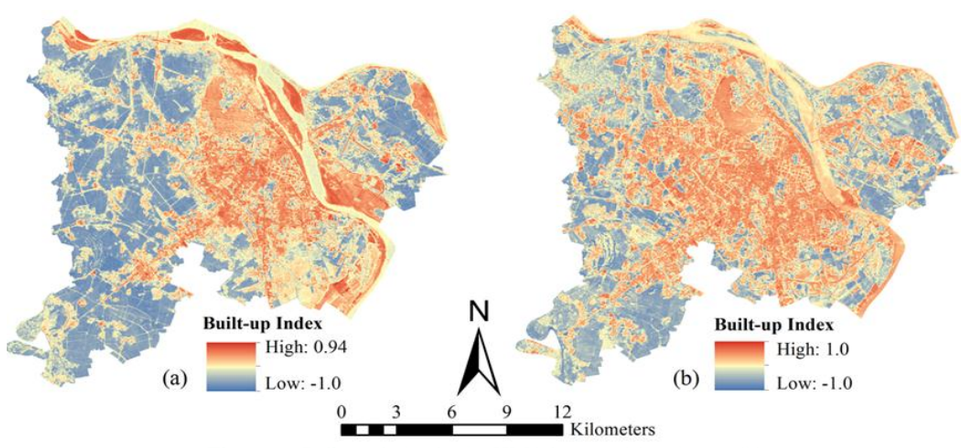

Figure-4. Built-up index in the HMA in 1996 (a) and 2016 (b).

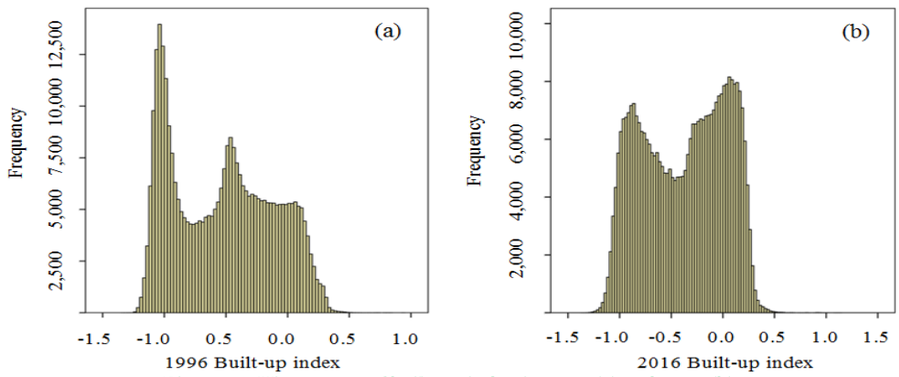

Figure-5. Histograms of built-up index in 1996 (a) and 2016 (b).

The distribution of the BU_c in the HMA on 10 June 1996 and 16 May 2016 are shown in Figures 4 and 5, whereas it's statistics are summarized in Table 1. Data from Figure 3 shows that similar to those of the NDBI, areas of low BU_c values were mainly detected in the western, north-western and south-western parts of the HMA at the two-time points, whereas, areas of high BU_c values were mainly concentrated in the core urban areas of the HMA. Data from Table 1 demonstrates BU_c ranged from -1 to 1 at the two-time points. The mean values of 0.53 in 1996 and 0.58 in 2016 proves built-up land had decreased during this period. Data from histograms in Figure 5 demonstrates that the distribution of the BU_c in 1996 was strongly right-skewed with many low BU_c values detected on the left of the histogram, especially for the negative BU_c values Figure 5-a. However, this trend had changed in 2016. Data in Figure 5-b demonstrates that the number of pixels with values greater than zero had increased much more than that of 1996. It is apparent that the values of the built-up index had increased dramatically during the period from 1996 to 2016.

4.3. Spatio-Temporal Changes of Built-Up Land During 1996-2016

Table-2. Summary of built-up land in the HMA during the period of 1996-2016.

Land cover	1996		2016	
	Area (ha)	Percent (%)	Area (ha)	Percent (%)
Built-up	4063.1	13.3	7163.2	23.4
Non-Built-up	26566.6	86.7	23466.4	76.6
Total	30629.6	100.0	30629.6	100.0

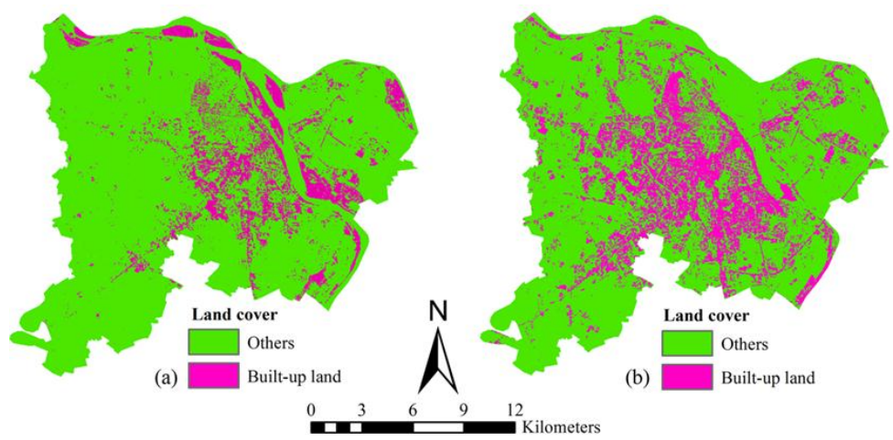

Figure-6. Built-up land in the HMA in 1996 (a) and 2016 (b).

The spatial distribution of urban built-up land in the HMA is shown in Figure 6, whereas, its statistics are summarized in Table 2. Data in Table 2 shows that the total urban built-up land area was 4063.1 hectares; accounting for 13.3% of the total area is 1996, while the non-built-up land area was 26566.6 hectares, accounting for 86.7% of the total area. The distribution of urban built-up land was mainly concentrated in the central HMA area Figure 6-a. The built-up land area had increased to 7163.2 hectares in 2016 which accounts for 23.4% of the total area. Data in Figure 6-b shows that the built-up land tends to expand to the west, southwest, and south of the HMA. Thus, the urban built-up land area had increased to about 10% of the total area in 20 years. A total of 0.5% of the built-up area increases on average each year. This result shows that HMA had experienced a fairly fast urbanization rate in the period of 1996-2016.

5. Conclusions

In this study, spatio-temporal analysis of built-up land changes in the HMA, Vietnam was investigated based on Landsat time-series images acquired in 1996 and 2016. Landsat remotely sensed images were first pre-processed using inflight sensor calibration parameters and atmospherically corrected using the FLAASH algorithm. Urban built-up land was then extracted based on the NDBI based continuous built-up index. Spatio-temporal changes of built-up land were finally analyzed and statistically summarized with the help of GIS. The study results show that the built-up land area had increased from 4063.1 ha to 7163.2 ha in June 1996 and May 2016 which account for 13.3% and 23.4% of the total area, respectively. The urban built-up land area had increased about 10.1% of the total area in

20 years and tends to expand to the west, southwest, and south of the HMA. The results of this study demonstrate that spatio-temporal changes of urban built-up land can be effectively and quickly monitoring and assessed using remotely sensed images.

References

[1] Y. Zha, J. Gao, and S. Ni, "Use of normalized difference built-up index in automatically mapping urban areas from TM imagery," *International Journal of Remote Sensing*, vol. 24, pp. 583-594, 2003. Available at: https://doi.org/10.1080/01431160304987.

[2] H. Xu, "A new index for delineating built-up land features in satellite imagery," *International Journal of Remote Sensing*, vol. 29, pp. 4269-4276, 2008. Available at: https://doi.org/10.1080/01431160802039957.

[3] C. L. Zhang, F. Chen, S. G. Miao, Q. C. Li, X. A. Xia, and C. Y. Xuan, "Impacts of urban expansion and future green planting on summer precipitation in the Beijing metropolitan area," *Journal of Geophysical Research: Atmospheres*, vol. 114, pp. 1-26, 2009.

[4] J. Hu, Y. Liu, and Y.-F. Sang, "Precipitation complexity and its spatial difference in the Taihu Lake Basin, China," *Entropy*, vol. 21, pp. 1-12, 2019. Available at: https://doi.org/10.3390/e21010048.

[5] R. K. Kaufmann, K. C. Seto, A. Schneider, Z. Liu, L. Zhou, and W. Wang, "Climate response to rapid urban growth: Evidence of a human-induced precipitation deficit," *Journal of Climate*, vol. 20, pp. 2299-2306, 2007. Available at: https://doi.org/10.1175/jcli4109.1.

[6] M. Ranagalage, R. C. Estoque, and Y. Murayama, "An urban heat island study of the Colombo metropolitan area, Sri Lanka, based on Landsat data (1997–2017)," *ISPRS International Journal of Geo-Information*, vol. 6, pp. 1-17, 2017. Available at: https://doi.org/10.3390/ijgi6070189.

[7] J. Tan, Y. Zheng, X. Tang, C. Guo, L. Li, G. Song, X. Zhen, D. Yuan, A. J. Kalkstein, and F. Li, "The urban heat island and its impact on heat waves and human health in Shanghai," *International Journal of Biometeorology*, vol. 54, pp. 75-84, 2010. Available at: https://doi.org/10.1007/s00484-009-0256-x.

[8] L. Liu and Y. Zhang, "Urban heat island analysis using the Landsat TM data and ASTER data: A case study in Hong Kong," *Remote Sensing*, vol. 3, pp. 1535-1552, 2011. Available at: https://doi.org/10.3390/rs3071535.

[9] K. Ford, *Remote sensing for planners*. Rutgers, USA: Center for Urban Policy Research, 1979.

[10] D. Lindgren, *Land use planning and remote sensing* vol. 2. The Netherlands: Taylor & Francis, 1984.

[11] Q. Zhang, J. Wang, X. Peng, P. Gong, and P. Shi, "Urban built-up land change detection with road density and spectral information from multi-temporal Landsat TM data," *International Journal of Remote Sensing*, vol. 23, pp. 3057-3078, 2002.

[12] T. D. Vu and T. T. Nguyen, "Spatio-temporal changes of underground coal fires during 2008–2016 in Khanh Hoa coal field (North-east of Viet Nam) using Landsat time-series data," *Journal of Mountain Science*, vol. 15, pp. 2703-2720, 2018. Available at: https://doi.org/10.1007/s11629-018-4997-z.

[13] P. K. Gangopadhyay, K. Lahiri-Dutt, and K. Saha, "Application of remote sensing to identify coalfires in the Raniganj Coalbelt, India," *International Journal of Applied Earth Observation and Geoinformation*, vol. 8, pp. 188-195, 2006. Available at: https://doi.org/10.1016/j.jag.2005.09.001.

[14] J. Masek, F. Lindsay, and S. Goward, "Dynamics of urban growth in the Washington DC metropolitan area, 1973-1996, from Landsat observations," *International Journal of Remote Sensing*, vol. 21, pp. 3473-3486, 2000. Available at: https://doi.org/10.1080/014311600750037507.

[15] M. Kawamura, "Relation between social and environmental conditions in Colombo Sri Lanka and the urban index estimated by satellite remote sensing data," in *Proceeding 51st Annual Conference of the Japan Society of Civil Engineers*, 1996.

[16] A. As-syakur, I. Adnyana, I. W. Arthana, and I. W. Nuarsa, "Enhanced built-up and bareness index (EBBI) for mapping built-up and bare land in an urban area," *Remote Sensing*, vol. 4, pp. 2957-2970, 2012.

[17] D. Stathakis, K. Perakis, and I. Savin, "Efficient segmentation of urban areas by the VIBI," *International Journal of Remote Sensing*, vol. 33, pp. 6361-6377, 2012. Available at: https://doi.org/10.1080/01431161.2012.687842.

[18] C. He, P. Shi, D. Xie, and Y. Zhao, "Improving the normalized difference built-up index to map urban built-up areas using a semiautomatic segmentation approach," *Remote Sensing Letters*, vol. 1, pp. 213-221, 2010. Available at: https://doi.org/10.1080/01431161.2010.481681.

[19] A. Rasul, H. Balzter, G. R. F. Ibrahim, H. M. Hameed, J. Wheeler, B. Adamu, S. a. Ibrahim, and P. M. Najmaddin, "Applying built-up and bare-soil indices from landsat 8 to cities in dry climates," *Land*, vol. 7, pp. 1-13, 2018. Available at: https://doi.org/10.3390/land7030081.

[20] T. M. Nguyen, T.-H. Lin, and H.-P. Chan, "The environmental effects of urban development in Hanoi, Vietnam from satellite and meteorological observations from 1999–2016," *Sustainability*, vol. 11, pp. 1-24, 2019. Available at: https://doi.org/10.3390/su11061768.

[21] A. ESRI, *ArcMap10.2*. Redlands, California, USA: ESRI, 2014.

[22] T. D. Vu and T. T. Nguyen, "Remote sensing and GIS-based River Bank Accretion Erosion Assessment in the Confluence of Thao-Da-Lo Rivers, North East of Vietnam," *Environment Asia*, vol. 11, pp. 27-44, 2018a.

[23] S. M. Adler-Golden, M. W. Matthew, L. S. Bernstein, R. Y. Levine, A. Berk, S. C. Richtsmeier, P. K. Acharya, G. P. Anderson, J. W. Felde, and J. Gardner, "Atmospheric correction for shortwave spectral imagery based on MODTRAN4. Imaging Spectrometry V," in *International Society for Optics and Photonics*, 1999, pp. 61-69.

[24] A. Berk, G. P. Anderson, L. S. Bernstein, P. K. Acharya, H. Dothe, M. W. Matthew, S. M. Adler-Golden, J. H. Chetwynd Jr, S. C. Richtsmeier, and B. Pukall, "MODTRAN4 radiative transfer modeling for atmospheric correction," in *Optical Spectroscopic Techniques and Instrumentation for Atmospheric and Space Research III*, 1999, pp. 348-353.

[25] O. Orhan, S. Ekercin, and F. Dadaser-Celik, "Use of landsat land surface temperature and vegetation indices for monitoring drought in the Salt Lake Basin Area, Turkey," *The Scientific World Journal*, vol. 2014, pp. 1-11, 2014.

[26] W. S. Logan, "The cultural role of capital cities: Hanoi and Hue, Vietnam," *Pacific Affairs*, vol. 78, pp. 559-575, 2005. Available at: https://doi.org/10.5509/2005784559.